

Customize Your Own Paired Data via Few-shot Way

Jinshu Chen Bingchuan Li* Miao Hua Panpan Xu Qian He
ByteDance Inc.

{chenjinshu, libingchuan, huamiao, xupanpan, heqian}@bytedance.com

arXiv:2405.12490v1 [cs.CV] 21 May 2024

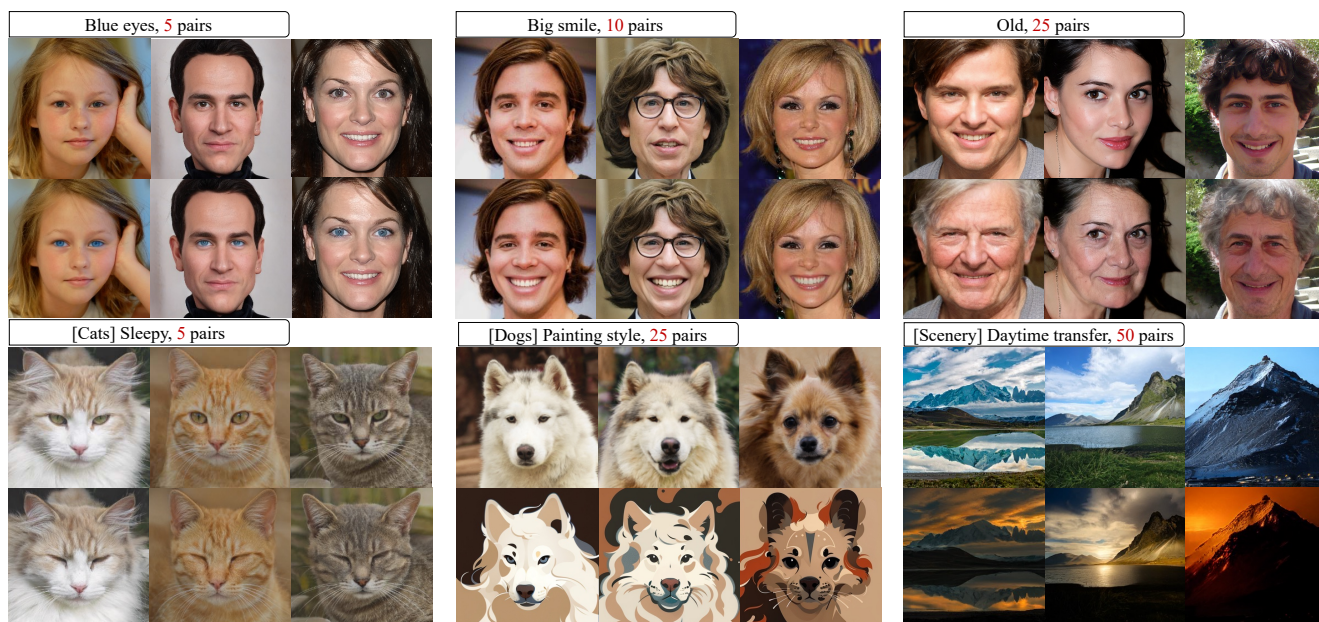


Figure 1. Providing only few source-target image pairs, users are allowed to efficiently customize their own image editing models through our framework. Without affecting irrelevant attributes, our proposed method can capture the desired effects precisely. Our model can handle various editing cases, whether the editing targets are commonly known concepts or completely newly defined by users.

Abstract

Existing solutions to image editing tasks suffer from several issues. Though achieving remarkably satisfying generated results, some supervised methods require huge amounts of paired training data, which greatly limits their usages. The other unsupervised methods take full advantage of large-scale pre-trained priors, thus being strictly restricted to the domains where the priors are trained on and behaving badly in out-of-distribution cases. The task we focus on is how to enable the users to customize their desired effects through only few image pairs. In our proposed framework, a novel few-shot learning mechanism based on the directional trans-

formations among samples is introduced and expands the learnable space exponentially. Adopting a diffusion model pipeline, we redesign the condition calculating modules in our model and apply several technical improvements. Experimental results demonstrate the capabilities of our method in various cases.

1. Introduction

Image editing is an important computer vision task which gives the user an interface with the generative models. Based on given instructions, editing models will transfer the original samples into the target domains by modifying certain aspects of the images. Attributes editing and stylizing are all

*Corresponding author

common examples of the image editing tasks.

Currently, image editing frameworks can be coarsely divided into several categories. As is widely acknowledged, editing tasks can be managed by paired-data-based supervised frameworks like [17, 26], since the original image and the image after edited can be seen as strictly paired data. Subsequently, a few unsupervised editing methods are introduced for the propose of editing images more easily and swiftly. Some proposed unsupervised methods operate directly in the latent space based on certain direction vectors[16, 29, 31, 56]. Recently, rapid advances in the field of multi-modal generation[19, 34–37] have led to new solutions to editing tasks. With the powerful pre-trained priors, such methods allow users to edit with raw sketches, a single reference image or only few words[4, 24, 28].

However, the existing editing methods all have shortcomings to some extent. Firstly, for the methods based on paired data, it is costly to collect a large high-quality paired dataset in most cases. Next, for the methods which edit images in the unsupervised way, bad disentanglement always accompanies with the found implicit directions among different domains, which further leads to unexpected editing effects and makes the editing process imprecise. As for the methods running based on the editing instructions and extra priors, the capabilities of such models are limited by the pre-trained priors as well. For example, frameworks with pre-trained language models such as CLIP [34] cannot handle targets which natural language fails to describe, i.e., users can hardly create new effects beyond the learned domains of provided priors. In a word, there remain difficulties to customize image editing effects expediently, precisely and arbitrarily.

In this work, we get back to the solutions based on paired data, since it is the most direct and reliable way. Given only few pairs of personalized images, we aim to ensure the users to customize their effects efficiently. We first introduce a novel learning mechanism to conquer the overfitting obstacles from which most models suffer when facing small datasets. Instead of training models upon image pairs, we train models upon the directional transformations among samples, thus we can expand the learnable space exponentially. Adopting a diffusion model pipeline, we bring in the pixel-level transformations as the conditions, and redesign the condition injection modules along with some technical improvements to achieve better generation qualities.

As Fig. 1 and Fig. 5 show, sufficient experimental results demonstrate the abilities of our proposed method. Achieving an equivalent performance, the amount of the requiring training data of our method is only about 1% of that required by existing paired-data-based methods. There is no disentanglement issue in our method, which means our model focuses on expected editing targets and overlooks other irrelevant attributes. Since running without any task-specific priors, the capability of our model is not limited whether the target

effects are commonly known or brand-new concepts created by the users. To summarize, our contributions are as follows:

- We propose a novel image editing framework, which is driven by only few pairs of data but leads to high-quality generated results. Our approach provides a convenient way for users to customize their own image editing effects.
- We introduce an efficient few-shot learning mechanism. By making the model learn upon intra-domain transformations rather than cross-domain samples, we expand the learnable space exponentially approximately, which greatly reduces the reliance on large training datasets.
- Based on a diffusion pipeline, we extend the forms of condition to pixel-space transformations and redesign the whole condition calculating module. Besides, we bring in several slight but effective technical improvements like adaptive noises, skip connections and frequency constraints to our model to achieve better generation qualities.
- We conduct various experiments to demonstrate the capacities of our framework. Whether it is an attribute editing task or a stylizing task, an entirely newly created effect or a usual effect, an editing task on faces or none-face examples, our model succeeds in completing image editing reliably. Experiments also show that our method outperforms its competitive peers.

2. Related Work

2.1. Generative models

Generative models continuously play an important role in various computer vision tasks. For a long time, GANs [9, 11, 33, 39, 53] have been the main paradigm in the field of image generation, which are able to effectively solve a wide range of important tasks like image in-painting [51, 54, 55], image-to-image translation [1, 3, 52] and image synthesis [6, 23, 44]. In recent years, diffusion models [5, 10, 14, 15, 20, 21, 25, 38, 46, 47] have been proposed as the new SOTA in terms of the generation quality. Adopting a stepwise noising-denoising design, the diffusion models have far finer generation qualities than other self-supervised methods especially on datasets with huge intra-domain variance [8, 42]. In this paper, based on a diffusion pipeline [36], we redesign the forms of conditions and the whole condition-calculating modules. To achieve high-quality image generation, we apply several simple but efficient improvements upon the basic framework.

2.2. Image editing

Various methods were proposed to solve the image editing tasks. There were a number of approaches [17, 26, 27, 41] that used the paired-data-based frameworks to solve the image editing tasks in early years. The introduction of StyleGAN [19] encouraged a number of distribution-based editing frameworks to be proposed [2, 7, 12, 29, 43, 48, 50]. Such

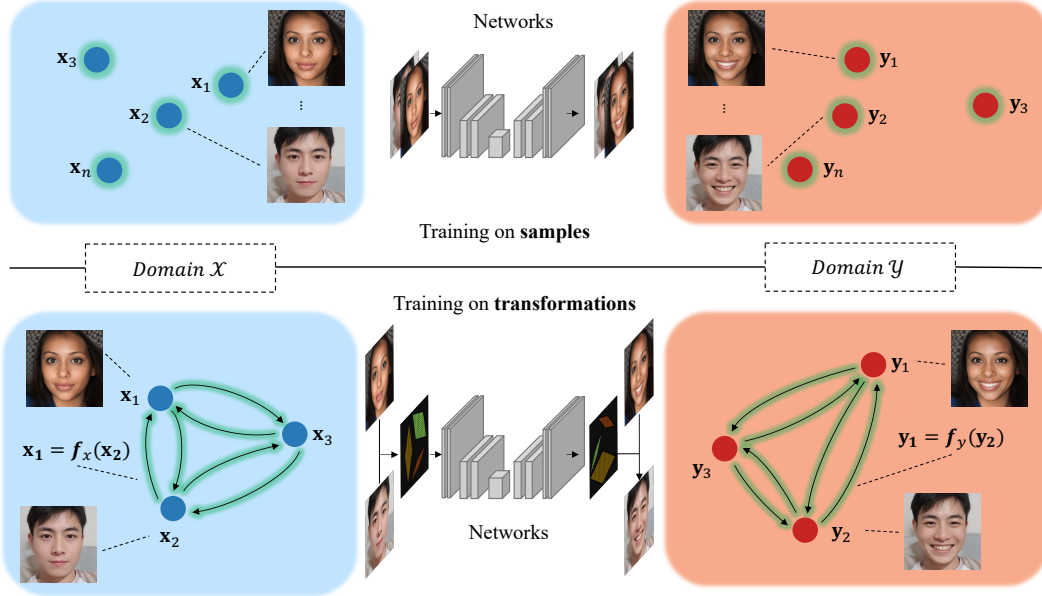


Figure 2. Instead of training the model on the paired samples themselves, we train the model on the directed transformations among samples from the same domain. In the figure we highlight the training objects in green to show the differences between ours and the existing method. In this way we expand the learnable space to an exponential extent approximately.

approaches calculate directed vectors between the source and target domains, then operate directly in the latent space, the modulation space or the parameter space based on the found directions. Recently, editing images with multi-modal information and pre-trained large models [4, 13, 24, 28, 31] has been widely accepted by users, and the editing instructions are no longer restricted to the form of images.

In this work, we return to editing images with paired-data, aiming to accomplish the task through a more cost-effective approach. We consider using paired data directly, which avoids the disentangling problems that may appear in the latent space or in the parameter space of the model. Besides, paired-data-based methods are far more suitable for customized image editing cases than methods using pre-trained models, as pre-trained models cannot manage tasks beyond their training domains. To conquer the heavy reliance on large paired dataset, we propose to expand the dataset itself rather than introducing any additional priors, which would avoid the model being limited by the capabilities imposed by the priors themselves.

3. Method

3.1. Expansion methods for few-shot datasets

Given the source domain \mathcal{X} and the target domain \mathcal{Y} , the editing model marked as M will be trained on pairs marked as $[\mathbf{x}, \mathbf{y}]$ where $\mathbf{x} \in \mathcal{X}$ and $\mathbf{y} \in \mathcal{Y}$. We can simply conclude the image editing task as training the model M to

fit the function $\mathbf{y} = M(\mathbf{x})$. We call such method of training on $[\mathbf{x}, \mathbf{y}]$ pairs “one-source-to-one-target” for short. Mark m as the total number of the training pairs, such training process works well when m is large. However, when it comes to the few-shot cases, M tends to overfitting the mapping relationships provided by little training data, because the learnable space of M is correlated with m only to a linear extent. Phenomenons like mode collapse indicate that when the generative model overfits, it has learned only few patterns and fails on samples outside the training domain.

We introduce a novel approach which expands the learnable space of the training dataset without bringing in any other class-related priors. Instead of training M on batches of paired data, we consider to make M train upon the transform function f , which conducts transformations **inside** the batches of paired data. Specifically, we can randomly sample n pairs of training data, marked as $\{[\mathbf{x}_1, \mathbf{y}_1], [\mathbf{x}_2, \mathbf{y}_2], \dots, [\mathbf{x}_n, \mathbf{y}_n]\}$, from the total training dataset with replacement. Among samples inside such group, obviously, there must be functions f_x and f_y which complete the one-to-the-other transformations, i.e., for $\forall i, 1 \leq i \leq n, i \in \mathbb{N}^+, \exists (f_x, f_y)$ satisfies $\mathbf{x}_i = f_x(\{\mathbf{x}_j\})$ and $\mathbf{y}_i = f_y(\{\mathbf{y}_j\})$, where $1 \leq j \leq n, j \neq i, j \in \mathbb{N}^+$.

Here we start off with the simplest case where $n = 2$. To construct each $\{[\mathbf{x}_1, \mathbf{y}_1], [\mathbf{x}_2, \mathbf{y}_2]\}$, given $[\mathbf{x}_1, \mathbf{y}_1]$, there will be C_m^1 additional $[\mathbf{x}_2, \mathbf{y}_2]$ to be selected from the training dataset. Namely, if we set the training target of M to fitting $f_y = M(f_x)$, there are $m * C_m^1$ pairs of $[f_x, f_y]$ for the model

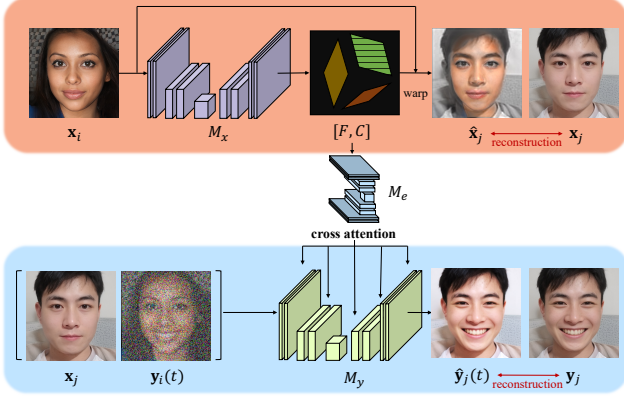


Figure 3. All modules of our framework are trained jointly and end-to-end. During training, all samples mentioned in the illustration are selected from the whole training dataset, while x_j is provided by users and will be transferred to get y_j for the inference time.

to learn from, which are far larger than the number of $[x, y]$, i.e., m . Fig. 2 is an illustration of $n = 2$ case. To distinguish from the “one-source-to-one-target” method, we call our method “ n -source-to- n -target”. n can be assigned to values larger than 2, and a larger n means the expansion’s degree of the training dataset is larger. The degree of expansion refers to $m * C_m^{n-1}$, which approximately leads to an exponential growth of the learnable space. We adopt the setting of $n = 2$ in all following statements and experiments, while a further discussion about other settings of n value is in the appendix.

Reasonability: Consider the simplest case: suppose that $\exists x_1, x_2$, x_2 is the version of x_1 after horizontally flipped, then the corresponding y_2 should be the version of y_1 after horizontally flipped as well. In this simple case, both f_x and f_y equal the function of horizontal flip, namely $f_x = f_y$. Similar conclusions can be drawn when f is simple spatial transform like vertical flip, rotation, padding and so on. In more general cases, the differences between two images often represent as different id information, different poses, etc., where f_x is unlikely to straightly equal to f_y . However, perceptually we find that complex transformations can always be decomposed into linear or non-linear combinations of fundamental transformation functions. Hence, there is certain manifold upon which the projections of f_x and f_y are equal. An illustration Fig. 4 is shown for the better understanding. The explanation mentioned above suggests that training M on (f_x, f_y) pairs is reasonable and able to converge.

3.2. Approach

We build two models, marked as M_x and M_y respectively, to calculate the transform relationships f_x and f_y . The overall model M runs to convert f_x to f_y . More precisely, we make M_x transform x_i to x_j , thus we obtain f_x . Due to the

relationships between f_x and f_y explained in Sec. 3.1, f_x can assist M_y to transform y_i to y_j , where y_j is exactly the edited target we need. All these models are trained jointly and the whole training process is end-to-end. For the training procedure, x_i, x_j, y_i and y_j are all randomly sampled from the training datasets. As for the test time, x_i, y_i are still random training samples, while x_j refers to the image need to be edited and y_j is the expected result. The complete framework is shown in Fig. 3.

In terms of the conversion among samples of the source domain \mathcal{X} , we simplify the transformation between two images to spatial transformations \mathcal{T}_s combined with color shifting \mathcal{T}_c , both of which are kinds of explicit representations. Inspired by existing methods [45], optical flow per pixel is chosen to embody spatial transforms \mathcal{T}_s . Mark a flow-field map as $F \in \mathbb{R}^{H \times W \times 2}$, where H, W equals the height and width of the image respectively. With the directions of the height H and width W used as the coordinate axes, $\forall h, w \in \mathbb{N}^+, 1 \leq h \leq H, 1 \leq w \leq W$, the value at the position of (h, w) , i.e., $F_{h,w} \in \mathbb{R}^2$, represents a set of positions in the reference image. Given a reference image I_{ref} , mark the warped image after applying F as I_{flow} . To calculate the value at each position of I_{flow} , get the value at the same position of F , treat such value of two dimensions as a set of coordinates, and assign the value from I_{ref} which locates in such coordinates to pixels of I_{flow} . Eq. (1) expresses the spatial transformation \mathcal{T}_s mentioned above.

$$I_{h,w}^{flow} = \mathcal{T}_s(I^{ref}) = I_{F_{(h,w)_1}, F_{(h,w)_2}}^{ref} \quad (1)$$

As for color shifting \mathcal{T}_c , we use 2D linear affine transformations marked as $C \in \mathbb{R}^{H \times W \times 2}$, where $C_{h,w} \in \mathbb{R}^2$ denotes a set of affine parameters. In particular, given a reference image I_{ref} , mark the version of I_{ref} after affine transformed as I_{aff} , then the color shifting \mathcal{T}_c can be calculated as Eq. (2).

$$I_{h,w}^{aff} = \mathcal{T}_c(I^{ref}) = C_{(h,w)_1} * I_{h,w}^{ref} + C_{(h,w)_2} \quad (2)$$

According to the above explanation, M_x takes in x_i and outputs a set of transformations containing F and C . Applying F and C to x_i in sequence, we obtain the predicted result \hat{x}_j , which is described in Eq. (3).

$$\hat{x}_j = \mathcal{T}_c(\mathcal{T}_s(x_i)) \quad (3)$$

By setting pixel-level reconstruction loss like MSE between \hat{x}_j and x_j , M_x is trained to finish the image editing task in the source domain, whose output marked as $[F, C] \in \mathbb{R}^{H \times W \times 4}$ represents the explicit transformations between \hat{x}_j and x_j , i.e., f_x .

Compared with the conversion among images of the source domain \mathcal{X} , the translation in the target domain \mathcal{Y} is what we really care about in editing tasks. To ensure the

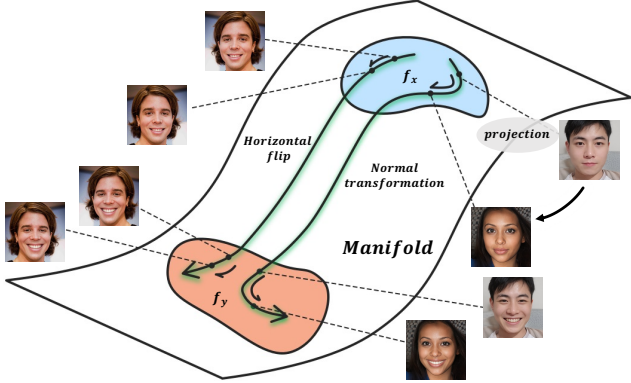


Figure 4. Essentially, our model is trained to find certain manifold where the projections of f_x and f_y are equal. Horizontal flip is shown on the upper left as a simple example, and normal cases are shown on the lower right.

high qualities of the edited results y_j , we adopt a diffusion pipeline to train M_y . The way of adding noises of the pipeline obeys a regular linear approach. The value of t varies during training. Hyperparameters related to t determine the degree of noise added to the image. A noise marked as z is randomly sampled from the Gaussian distribution $\mathcal{N}(0, I)$. The final time-specific results combined by y_i and z is marked as $y_i(t)$. Furthermore, we concatenate x_j to $y_i(t)$ and treat such $y_i(t)|x_j$ as the input of M_y , which makes the whole training process of the framework more stable.

A difference between ours and other methods is the training target of M_y is to reconstruct neither $y_i(0)$ nor z but y_j . $[F, C]$ is considered as condition information besides x_j , which will act on M_y through cross-attention modules after passing an additional embedding module marked as M_e . A discussion about this algorithm part is in our appendix.

3.3. Technical details and improvements

Our overall framework is inspired by [36]: M_y runs between a pair of encoder-decoder, which makes the framework work in the semantic space. There are two kinds of conditions in our framework, one is x_i which works by concatenation, and the other is $M_e([F, C])$ coming from M_x which works through cross-attention modules.

We notice that some methods use frozen pre-trained encoder-decoder, i.e., a variational auto-encoder or VAE [32] namely, in their diffusion models when training from the scratch or fine-tuning on their customized tasks. Such VAEs are well-trained on huge datasets along with traditional distribution-based and reconstruction losses. However, VAEs are always criticized for blurred and oversmoothing generated images. Then some existing methods conducting an extra online super-resolution behind the output of the decoder as a remedy. In our approach, we take the follow-

ing steps to achieve high-quality image generation directly: Train the VAE together with the other parts of the framework without freezing any parameters, add adaptive noises to the intermediate layers of the decoder and set skip connections between relative layers of the encoder and the decoder.

Since small datasets have a far stronger bias than huge datasets, the knowledge learned from huge datasets[8] may be inappropriate for training models in customized few-shot cases. We treat the VAE as a trainable sub-module, which acts like not “semantic” compressing but only “dimension” compressing, then the VAE is more likely to adjust to the specific cases provided by the users. Adding noises and skip connections are common approaches in existing methods [19]. We observe that these two tricks enable the model to capture the high frequency information, thus increasing the details of the generated samples to a large extent.

Additionally, following Dits [30], we replace the backbone U-Net of M_y with ViTs [49] and add dual layer normalization layers [22], by which we observe an improvement on the quality of generated samples. To further enhance the generalization of the model, we apply augmentation methods to x_j and y_j . Augmentations we use include horizontal flip, color jitter and random affine, which are all common in existing frameworks. Moreover, a constraint in the frequency domain [18] is applied which makes the model coverage faster and perform better especially in details.

4. Experiments

4.1. Generated results

Generated results of our framework are shown in Fig. 1 and Fig. 5. The editing targets and the amount of given training data pairs are recorded on the top of each result unit in the figure, and the relative generated samples are shown below. Our experiments are conducted on both 256px and 512px. To thoroughly test the capability of the model, experiments are carried out on a wide field of topics. More visual results, training hyper-parameters, detailed experimental settings, experiments about proper m value for different topics, and a discussion about the limitations of our method are shown in our appendix.

4.2. Comparison

We roughly divide the competitive peers of our method into two types: paired data based methods and unpaired data based methods, according to whether using paired training data. For comparing with methods that training with paired data, we primarily care about the trade-off between the generated qualities and the number of training samples. For comparing with methods that are independent of paired data, we will show different performances of mentioned methods with comparable data costs. For all the baselines, we use the source codes and parameter settings released officially.



Figure 5. Here we show more experimental results of our method. The editing target and the amount of given training pairs are recorded on the top of each result unit, and the relative generated images are displayed below. More visual results are shown in our appendix.

Evaluation settings. For each experiment of the fair comparison, we firstly run all the methods through different amounts of training data in order to find out how much paired data is needed for each method to behave best. Be-

sides recording the performances got on an adequate amount, we record the results of the competitors when they run with the same amount of data as ours for a more clear comparison. For the unfair comparison, we provide proper samples

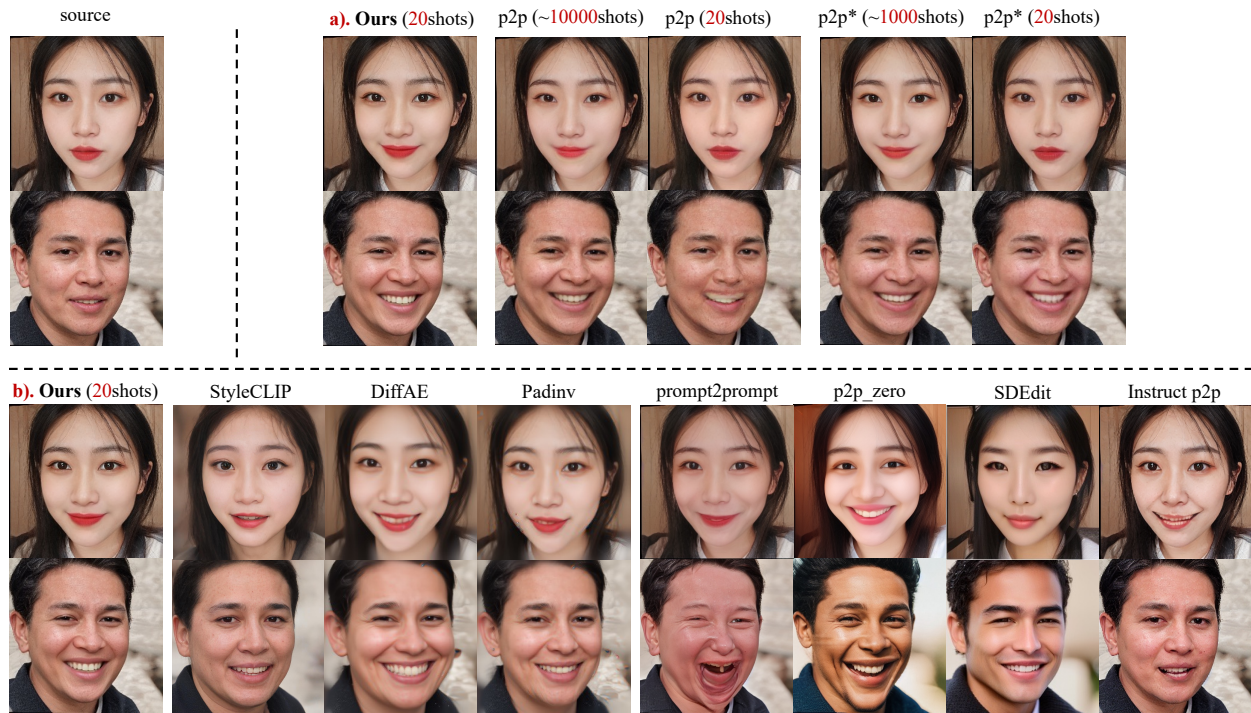


Figure 6. Comparisons between existing works and our method. Part **a)** shows comparisons with paired-data methods, while part **b)** contains results comparing with few/zero-shot methods including methods editing in the latent space and methods relying on the multi-modal information. Note that for the latter methods, we will provide proper instructions which can describe the editing target.

according to the actual needs of the methods, and we test the performances of our framework with comparable data costs.

Metrics. There are several criteria used when comparing performances. Firstly, FID [40] is calculated to measure the similarity between the generated samples and the real ones. Furthermore, to measure the degree of clarity, PSNR is calculated. Moreover, we introduce another metric named DIOU in the case of available paired data. Given a pair of samples, we can obtain the editing targets by subtracting the source image from its paired target image directly in the pixel space. Finding the unions of all editing target areas of the training data, we can assign it as the expected targets of the total task. In a similar way we can calculate the actual edited areas generated by the model. Then the intersection over those two kinds of unions, namely IoU, may represent the “accuracy” of the model when editing images. A lower DIOU, the IoU of Diversities generated by the model, means the model learns the editing targets more precisely.

Main conclusions. The qualitative results are shown in Fig. 6 and quantitative results are in Tab. 1. As a more general evaluation, the user study is shown in our appendix.

For the part of fair comparisons, we train pix2pix [17], pix2pix* and our method upon a number of different editing cases. Note that pix2pix* is an improved version of pix2pix with a few technical tricks whose detailed settings can be

found in the appendix. Obviously, our method can achieve an equivalent performance compared to its competitive peers with only 10% or even 1% of the training samples. Such amounts of samples are absolutely affordable when users hope to customize their own image editing tasks. A further comparison about the training time is in the appendix.

For the experiments of unfair comparisons, we select a series of methods to compare with including DiffAE [31], Styleclip [29], Padinv [2], prompt2prompt [13], pix2pix-zero [28], SDEdit [24] and instruct-pix2pix [4]. We choose these editing methods to compare with because they all run with little data cost. However, it is worth emphasizing that these methods use strong priors like large well-trained models and are independent of paired samples, so they are not strictly competitive peers of our method. Actually for such methods editing in the domain level, disentanglement has been widely acknowledged as a troublesome problem. If the editing tasks require fine-grained operations, these methods tend to producing unexpected changes beyond the editing areas. Moreover, these frameworks can only fetch and combine **known** concepts from the priors’ training spaces, which means users can hardly **create** their own effects from scratch. As Fig. 6 shows, visually, our method manages to handle few-shot cases. Furthermore, areas outside the editing targets preserve quite well in our generated samples. As our

Methods	FID↓	PSNR↑	DIoU↑
Pix2pix-20shots	0.2971	17.9045	0.8253
Pix2pix~10000shots	0.0176	24.5218	0.8755
Pix2pix*-20shots	0.1882	20.0071	0.8401
Pix2pix*~1000shots	0.0151	26.6419	0.9037
StyleCLIP	0.0332	27.4288	0.6506
DiffAE	0.2580	27.5360	0.7476
Padinv	0.0721	27.1953	0.7380
prompt2prompt	0.4725	27.0361	0.5628
pix2pix-zero	0.3617	27.8343	0.5054
SDEdit	0.1764	27.4527	0.6822
Instruct-pix2pix	0.1490	27.1438	0.7779
Ours-20shots	0.0094	27.8455	0.9352

Table 1. The quantitative results between ours and existing methods. The metrics are calculated on 1000 randomly generated samples. All values recorded in the table are averages across multi-repeating experiments.

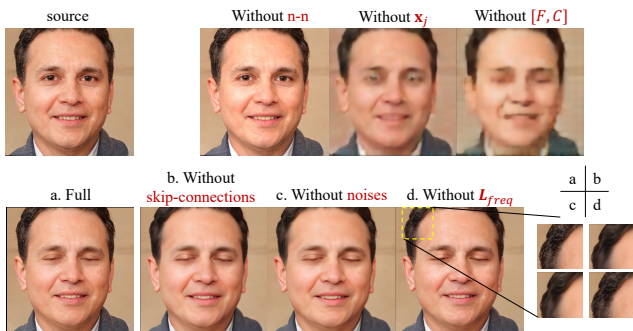


Figure 7. The qualitative results of the ablation study. Without our “ n -source-to- n -target” method, the model overfits easily. Both \mathbf{x}_j and $[F, C]$ ease the difficulties of the training. The improvements we adopt help the model to generate more fine-grained results.

framework runs without any priors, there are no restrictions on the capacities of the model.

5. Ablation study

5.1. Effects of the data pairing mechanism

As Sec. 3.1 explains, the expansion method is the key to make the whole framework run with few samples. We set a pair of experiments, one of which is the original model we proposed, and the other returns to a normal “one-source-to-one-target” methods like ways used in existing models, i.e., both M_x and M_y take in \mathbf{x}_i and output \mathbf{y}_i . Results in Fig. 7 and Tab. 2 show that the “one-source-to-one-target” method gets stuck in overfitting easily with few training samples, while our “ n -source-to- n -target” method runs stably.

Setting	FID↓	PSNR↑	DIoU↑
Baseline	0.0094	27.8455	0.9352
without “ $n - n$ ”	0.9635	20.6481	0.2830
without \mathbf{x}_j	0.5502	17.5893	0.1894
without $[F, C]$	0.6938	17.2037	0.2043
without skip-connections	0.0256	25.4526	0.3451
without noises	0.0127	26.4819	0.7129
without L_{freq}	0.0115	26.9471	0.8125

Table 2. The quantitative results of the ablation study. Recorded values are consistent with conclusions drawn from Fig. 7.

5.2. Effects of the condition

There are two kinds of condition in our framework: \mathbf{x}_j concatenated to $\mathbf{y}_i(t)$, and $[F, C]$ output by M_x . The first experiment is conducted to observe the influence if \mathbf{x}_j is not provided as a condition. As Fig. 7 shows, \mathbf{x}_j greatly decreases the difficulties of the training process, making the model converge more easily. The second experiment aims to evaluate the effects of $[F, C]$. We disable $M_e[F, C]$ by setting the input conditions of cross attention module to a constant and train the whole model, which forces the model to train to fit \mathbf{y}_j only based on $\mathbf{y}_i(t)$ and \mathbf{x}_j . Without a proper guidance, we observe a similar phenomenon that the model is hard to converge. Especially, it takes a much longer time for M_y to generate the overall contour shape of \mathbf{y}_j . Finally we draw the conclusion that such two conditions provide a basic “canvas”, thus the model only need to focus on the differences between domain \mathcal{X} and domain \mathcal{Y} .

5.3. Ablation study of the technical tricks

We set a few experiments to figure out the actual effect of each technical tricks. As Fig. 7 shows, adding skip connections assists the model in generating details, while adding noises and applying frequency loss work similarly to enrich the information in extremely high frequency domains. The subplot on the bottom right of Fig. 7 shows the different performances of the mentioned methods in generating high frequency details.

6. Conclusion

We propose a novel framework which encourages users to customize their own editing models with only few pairs of training data. Our model is based on an efficient dataset expansion method, a robust diffusion pipeline, a few re-designed modules and technical improvements. Experiments demonstrate that our model is able to handle different topics of editing tasks and has good qualities of generated images. Further discussions about limitations, future work, and other details are shown in the appendix.

References

- [1] Ivan Anokhin, Pavel Solovev, Denis Korzhenkov, Alexey Kharlamov, Taras Khakhulin, Aleksei Silvestrov, Sergey Nikolenko, Victor Lempitsky, and Gleb Sterkin. High-resolution daytime translation without domain labels. In *Proceedings of the IEEE/CVF Conference on Computer Vision and Pattern Recognition*, pages 7488–7497, 2020. [2](#)
- [2] Qingyan Bai, Yinghao Xu, Jiapeng Zhu, Weihao Xia, Yujie Yang, and Yujun Shen. High-fidelity gan inversion with padding space. In *European Conference on Computer Vision*, pages 36–53. Springer, 2022. [2](#), [7](#)
- [3] Deblina Bhattacharjee, Seungryong Kim, Guillaume Vezier, and Mathieu Salzmann. Dunit: Detection-based unsupervised image-to-image translation. In *Proceedings of the IEEE/CVF Conference on Computer Vision and Pattern Recognition*, pages 4787–4796, 2020. [2](#)
- [4] Tim Brooks, Aleksander Holynski, and Alexei A Efros. Instructpix2pix: Learning to follow image editing instructions. *arXiv preprint arXiv:2211.09800*, 2022. [2](#), [3](#), [7](#)
- [5] Nanxin Chen, Yu Zhang, Heiga Zen, Ron J Weiss, Mohammad Norouzi, and William Chan. Wavegrad: Estimating gradients for waveform generation. *arXiv preprint arXiv:2009.00713*, 2020. [2](#)
- [6] Yunjey Choi, Youngjung Uh, Jaejun Yoo, and Jung-Woo Ha. Stargan v2: Diverse image synthesis for multiple domains. In *Proceedings of the IEEE/CVF conference on computer vision and pattern recognition*, pages 8188–8197, 2020. [2](#)
- [7] Edo Collins, Raja Bala, Bob Price, and Sabine Susstrunk. Editing in style: Uncovering the local semantics of gans. In *Proceedings of the IEEE/CVF Conference on Computer Vision and Pattern Recognition*, pages 5771–5780, 2020. [2](#)
- [8] Jia Deng, Wei Dong, Richard Socher, Li-Jia Li, Kai Li, and Li Fei-Fei. Imagenet: A large-scale hierarchical image database. In *2009 IEEE conference on computer vision and pattern recognition*, pages 248–255. Ieee, 2009. [2](#), [5](#)
- [9] Emily L Denton, Soumith Chintala, Rob Fergus, et al. Deep generative image models using a laplacian pyramid of adversarial networks. *Advances in neural information processing systems*, 28, 2015. [2](#)
- [10] Prafulla Dhariwal and Alexander Nichol. Diffusion models beat gans on image synthesis. *Advances in Neural Information Processing Systems*, 34:8780–8794, 2021. [2](#)
- [11] Ian Goodfellow, Jean Pouget-Abadie, Mehdi Mirza, Bing Xu, David Warde-Farley, Sherjil Ozair, Aaron Courville, and Yoshua Bengio. Generative adversarial networks. *Communications of the ACM*, 63(11):139–144, 2020. [2](#)
- [12] Erik Härkönen, Aaron Hertzmann, Jaakko Lehtinen, and Sylvain Paris. Ganspace: Discovering interpretable gan controls. *Advances in Neural Information Processing Systems*, 33:9841–9850, 2020. [2](#)
- [13] Amir Hertz, Ron Mokady, Jay Tenenbaum, Kfir Aberman, Yael Pritch, and Daniel Cohen-Or. Prompt-to-prompt image editing with cross attention control. *arXiv preprint arXiv:2208.01626*, 2022. [3](#), [7](#)
- [14] Jonathan Ho, Ajay Jain, and Pieter Abbeel. Denoising diffusion probabilistic models. *Advances in Neural Information Processing Systems*, 33:6840–6851, 2020. [2](#)
- [15] Jonathan Ho, Chitwan Saharia, William Chan, David J Fleet, Mohammad Norouzi, and Tim Salimans. Cascaded diffusion models for high fidelity image generation. *J. Mach. Learn. Res.*, 23(47):1–33, 2022. [2](#)
- [16] Minyoung Huh, Richard Zhang, Jun-Yan Zhu, Sylvain Paris, and Aaron Hertzmann. Transforming and projecting images into class-conditional generative networks. In *Computer Vision—ECCV 2020: 16th European Conference, Glasgow, UK, August 23–28, 2020, Proceedings, Part II 16*, pages 17–34. Springer, 2020. [2](#)
- [17] Phillip Isola, Jun-Yan Zhu, Tinghui Zhou, and Alexei A Efros. Image-to-image translation with conditional adversarial networks. In *Proceedings of the IEEE conference on computer vision and pattern recognition*, pages 1125–1134, 2017. [2](#), [7](#)
- [18] Liming Jiang, Bo Dai, Wayne Wu, and Chen Change Loy. Focal frequency loss for image reconstruction and synthesis. In *Proceedings of the IEEE/CVF International Conference on Computer Vision*, pages 13919–13929, 2021. [5](#)
- [19] Tero Karras, Samuli Laine, and Timo Aila. A style-based generator architecture for generative adversarial networks. In *Proceedings of the IEEE/CVF conference on computer vision and pattern recognition*, pages 4401–4410, 2019. [2](#), [5](#)
- [20] Diederik Kingma, Tim Salimans, Ben Poole, and Jonathan Ho. Variational diffusion models. *Advances in neural information processing systems*, 34:21696–21707, 2021. [2](#)
- [21] Zhifeng Kong, Wei Ping, Jiaji Huang, Kexin Zhao, and Bryan Catanzaro. Diffwave: A versatile diffusion model for audio synthesis. *arXiv preprint arXiv:2009.09761*, 2020. [2](#)
- [22] Manoj Kumar, Mostafa Dehghani, and Neil Houlsby. Dual patchnorm. *arXiv preprint arXiv:2302.01327*, 2023. [5](#)
- [23] Cheng-Han Lee, Ziwei Liu, Lingyun Wu, and Ping Luo. Maskgan: Towards diverse and interactive facial image manipulation. In *Proceedings of the IEEE/CVF Conference on Computer Vision and Pattern Recognition*, pages 5549–5558, 2020. [2](#)
- [24] Chenlin Meng, Yang Song, Jiaming Song, Jiajun Wu, Jun-Yan Zhu, and Stefano Ermon. Sdedit: Image synthesis and editing with stochastic differential equations. *arXiv preprint arXiv:2108.01073*, 2021. [2](#), [3](#), [7](#)
- [25] Gautam Mittal, Jesse Engel, Curtis Hawthorne, and Ian Simon. Symbolic music generation with diffusion models. *arXiv preprint arXiv:2103.16091*, 2021. [2](#)
- [26] Taesung Park, Ming-Yu Liu, Ting-Chun Wang, and Jun-Yan Zhu. Semantic image synthesis with spatially-adaptive normalization. In *Proceedings of the IEEE/CVF conference on computer vision and pattern recognition*, pages 2337–2346, 2019. [2](#)
- [27] Taesung Park, Ming-Yu Liu, Ting-Chun Wang, and Jun-Yan Zhu. Semantic image synthesis with spatially-adaptive normalization. In *Proceedings of the IEEE/CVF conference on computer vision and pattern recognition*, pages 2337–2346, 2019. [2](#)
- [28] Gaurav Parmar, Krishna Kumar Singh, Richard Zhang, Yijun Li, Jingwan Lu, and Jun-Yan Zhu. Zero-shot image-to-image translation. *arXiv preprint arXiv:2302.03027*, 2023. [2](#), [3](#), [7](#)
- [29] Or Patashnik, Zongze Wu, Eli Shechtman, Daniel Cohen-Or, and Dani Lischinski. Styleclip: Text-driven manipulation of

- stylegan imagery. In *Proceedings of the IEEE/CVF International Conference on Computer Vision*, pages 2085–2094, 2021. 2, 7
- [30] William Peebles and Saining Xie. Scalable diffusion models with transformers. *arXiv preprint arXiv:2212.09748*, 2022. 5
- [31] Konpat Preechakul, Nattanat Chatthee, Suttisak Widadwongsa, and Supasorn Suwajanakorn. Diffusion autoencoders: Toward a meaningful and decodable representation. In *Proceedings of the IEEE/CVF Conference on Computer Vision and Pattern Recognition*, pages 10619–10629, 2022. 2, 3, 7
- [32] Yunchen Pu, Zhe Gan, Ricardo Henao, Xin Yuan, Chunyuan Li, Andrew Stevens, and Lawrence Carin. Variational autoencoder for deep learning of images, labels and captions. *Advances in neural information processing systems*, 29, 2016. 5
- [33] Alec Radford, Luke Metz, and Soumith Chintala. Unsupervised representation learning with deep convolutional generative adversarial networks. *arXiv preprint arXiv:1511.06434*, 2015. 2
- [34] Alec Radford, Jong Wook Kim, Chris Hallacy, Aditya Ramesh, Gabriel Goh, Sandhini Agarwal, Girish Sastry, Amanda Askell, Pamela Mishkin, Jack Clark, et al. Learning transferable visual models from natural language supervision. In *International conference on machine learning*, pages 8748–8763. PMLR, 2021. 2
- [35] Aditya Ramesh, Prafulla Dhariwal, Alex Nichol, Casey Chu, and Mark Chen. Hierarchical text-conditional image generation with clip latents. *arXiv preprint arXiv:2204.06125*, 2022.
- [36] Robin Rombach, Andreas Blattmann, Dominik Lorenz, Patrick Esser, and Björn Ommer. High-resolution image synthesis with latent diffusion models. In *Proceedings of the IEEE/CVF Conference on Computer Vision and Pattern Recognition*, pages 10684–10695, 2022. 2, 5
- [37] Chitwan Saharia, William Chan, Saurabh Saxena, Lala Li, Jay Whang, Emily Denton, Seyed Kamyar Seyed Ghasemipour, Burcu Karagol Ayan, S Sara Mahdavi, Rapha Gontijo Lopes, et al. Photorealistic text-to-image diffusion models with deep language understanding. *arXiv preprint arXiv:2205.11487*, 2022. 2
- [38] Chitwan Saharia, Jonathan Ho, William Chan, Tim Salimans, David J Fleet, and Mohammad Norouzi. Image super-resolution via iterative refinement. *IEEE Transactions on Pattern Analysis and Machine Intelligence*, 2022. 2
- [39] Tim Salimans, Ian Goodfellow, Wojciech Zaremba, Vicki Cheung, Alec Radford, and Xi Chen. Improved techniques for training gans. *Advances in neural information processing systems*, 29, 2016. 2
- [40] Tim Salimans, Ian Goodfellow, Wojciech Zaremba, Vicki Cheung, Alec Radford, and Xi Chen. Improved techniques for training gans. *Advances in neural information processing systems*, 29, 2016. 7
- [41] Patsorn Sangkloy, Jingwan Lu, Chen Fang, Fisher Yu, and James Hays. Scribbler: Controlling deep image synthesis with sketch and color. In *Proceedings of the IEEE conference on computer vision and pattern recognition*, pages 5400–5409, 2017. 2
- [42] Christoph Schuhmann, Richard Vencu, Romain Beaumont, Robert Kaczmarczyk, Clayton Mullis, Aarush Katta, Theo Coombes, Jenia Jitsev, and Aran Komatsuzaki. Laion-400m: Open dataset of clip-filtered 400 million image-text pairs. *arXiv preprint arXiv:2111.02114*, 2021. 2
- [43] Yujun Shen, Jinjin Gu, Xiaoou Tang, and Bolei Zhou. Interpreting the latent space of gans for semantic face editing. In *Proceedings of the IEEE/CVF conference on computer vision and pattern recognition*, pages 9243–9252, 2020. 2
- [44] Assaf Shocher, Yossi Gandelsman, Inbar Mosseri, Michal Yarom, Michal Irani, William T Freeman, and Tali Dekel. Semantic pyramid for image generation. In *Proceedings of the IEEE/CVF Conference on Computer Vision and Pattern Recognition*, pages 7457–7466, 2020. 2
- [45] Aliaksandr Siarohin, Stéphane Lathuilière, Sergey Tulyakov, Elisa Ricci, and Nicu Sebe. First order motion model for image animation. *Advances in Neural Information Processing Systems*, 32, 2019. 4
- [46] Jascha Sohl-Dickstein, Eric Weiss, Niru Maheswaranathan, and Surya Ganguli. Deep unsupervised learning using nonequilibrium thermodynamics. In *International Conference on Machine Learning*, pages 2256–2265. PMLR, 2015. 2
- [47] Yang Song, Jascha Sohl-Dickstein, Diederik P Kingma, Abhishek Kumar, Stefano Ermon, and Ben Poole. Score-based generative modeling through stochastic differential equations. *arXiv preprint arXiv:2011.13456*, 2020. 2
- [48] Ayush Tewari, Mohamed Elgharib, Gaurav Bharaj, Florian Bernard, Hans-Peter Seidel, Patrick Pérez, Michael Zollhofer, and Christian Theobalt. Stylerig: Rigging stylegan for 3d control over portrait images. In *Proceedings of the IEEE/CVF Conference on Computer Vision and Pattern Recognition*, pages 6142–6151, 2020. 2
- [49] Ashish Vaswani, Noam Shazeer, Niki Parmar, Jakob Uszkoreit, Llion Jones, Aidan N Gomez, Łukasz Kaiser, and Illia Polosukhin. Attention is all you need. *Advances in neural information processing systems*, 30, 2017. 5
- [50] Zongze Wu, Dani Lischinski, and Eli Shechtman. Stylespace analysis: Disentangled controls for stylegan image generation. In *Proceedings of the IEEE/CVF Conference on Computer Vision and Pattern Recognition*, pages 12863–12872, 2021. 2
- [51] Zili Yi, Qiang Tang, Shekoofeh Azizi, Daesik Jang, and Zhan Xu. Contextual residual aggregation for ultra high-resolution image inpainting. In *Proceedings of the IEEE/CVF conference on computer vision and pattern recognition*, pages 7508–7517, 2020. 2
- [52] Pan Zhang, Bo Zhang, Dong Chen, Lu Yuan, and Fang Wen. Cross-domain correspondence learning for exemplar-based image translation. In *Proceedings of the IEEE/CVF Conference on Computer Vision and Pattern Recognition*, pages 5143–5153, 2020. 2
- [53] Junbo Zhao, Michael Mathieu, and Yann LeCun. Energy-based generative adversarial network. *arXiv preprint arXiv:1609.03126*, 2016. 2
- [54] Lei Zhao, Qihang Mo, Sihuan Lin, Zhizhong Wang, Zhiwen Zuo, Haibo Chen, Wei Xing, and Dongming Lu. Uctgan: Diverse image inpainting based on unsupervised cross-space

translation. In *Proceedings of the IEEE/CVF conference on computer vision and pattern recognition*, pages 5741–5750, 2020. 2

- [55] Chuanxia Zheng, Tat-Jen Cham, and Jianfei Cai. Pluralistic image completion. In *Proceedings of the IEEE/CVF Conference on Computer Vision and Pattern Recognition*, pages 1438–1447, 2019. 2
- [56] Jun-Yan Zhu, Philipp Krähenbühl, Eli Shechtman, and Alexei A Efros. Generative visual manipulation on the natural image manifold. In *Computer Vision—ECCV 2016: 14th European Conference, Amsterdam, The Netherlands, October 11–14, 2016, Proceedings, Part V 14*, pages 597–613. Springer, 2016. 2